DESIGN AND SIMULATION ANALYSIS OF LIGHTWEIGHT CLAMPING AND CONVEYING DEVICE FOR TOBACCO TOPPING

烟草打顶夹持输送装置设计与仿真分析

Fanting KONG¹⁾, Qing XIE *1), Yong LIN*2), Dexing SHI²⁾, Wei LIN²⁾, Jingchao LI²⁾, Xiaolong LI²⁾, Teng WU¹⁾, Yongfei SUN¹⁾, Changlin CHEN¹⁾

¹⁾ Nanjing Institute of Agricultural Mechanization, Ministry of Agriculture and Rural Affairs, Nanjing 210014/China;
²⁾ Nanping Branch of Fujian Tobacco Company, Nanping 353000/China
Tel: +86-15366092846; E-mail: xieqing431@126.com
Corresponding author: Qin Xie
DOI: https://doi.org/10.35633/inmateh-77-32

Keywords: agricultural machinery, experimentation, dynamic analysis, clamping conveyance

ABSTRACT

To meet the requirements of tobacco topping and ensure the efficient removal of topped buds, leaves, and shoots from the field. A lightweight clamping conveyor device was designed through an analysis of the forces acting on critical components and their operational principles. A rigid-flexible coupling dynamic simulation of the tobacco top stalks clamping and conveying process was conducted using ADAMS. An orthogonal experiment with three factors (forward speed, clamping distance, and conveying speed) at three levels was performed, with clamping success rate and conveying success rate as evaluation indices. Field validation experiments showed that at a forward speed of 0.6 m/s, a clamping distance of 11 mm, and a conveying speed of 1.1 m/s, the average clamping success rate was 94.52%, and the average conveying success rate was 98.36%. The conveying process was stable, with a high collection rate of top stalk, demonstrating strong adaptability to agricultural practices and meeting the operational requirements of tobacco topping in the field.

摘要

为满足烟草智能化打顶将打下的花蕾、叶、芽等清出田间的需求,现有智能切割打顶装备需配套可随切割装置快速移动的轻型夹持输送装置,防止输送过程中出现割下烟草顶花掉落、堵塞等问题,本研究通过对装置关键部件的受力及作业原理分析,并采用 ADAMS 开展夹持输送过程刚柔耦合动力学仿真,以前进速度、夹持间距、输送速度为试验因素进行三因素三水平的正交试验,以夹持成功率、输送成功率为评价指标确定最优参数组合。田间验证试验表明:烟草打顶机前进速度为 0.6 m/s,夹持间距为 11 mm,输送速度为 1.1 m/s 时,平均夹持成功率为 94.52%、平均输送成功率为 98.36%,输送过程平稳、顶花收集率高,对种植农艺适应性好,满足烟草打顶的田间作业要求。

INTRODUCTION

Tobacco is one of China's primary economic crops (Luo et al., 2023). Traditionally, tobacco cultivation and management have relied heavily on manual labour, which is costly, inefficient, and labour-intensive (Liu et al., 2016). Topping is a critical process in tobacco leaf production. Proper topping helps concentrate nutrients, meeting the growth needs of tobacco leaves, promoting leaf expansion and thickening, and ultimately enhancing both yield and quality (Lei et al., 2022). Research on tobacco topping machinery began earlier in foreign countries. In Europe and North America, large-scale, high-speed, and multifunctional equipment has been developed, with a trend toward precision operations and the integration of mechanical, electrical, and hydraulic systems (Worsham et al., 2002, Gravalos et al., 2019). In contrast, research in Asian countries such as Japan started later but has progressed rapidly, focusing on the development of specialized tobacco field equipment (Du et al., 2019). These countries have already developed standardized products that enable integrated operations for tobacco topping and sucker control. At present, research on tobacco topping machinery in China is relatively limited, and mechanized operations remain at a low level (Geng et al., 2010, Xia et al., 2017). With the increasing demand for automation and intelligence in agricultural production, the development of high-efficiency intelligent tobacco topping machinery has become a key research focus. Research is progressing toward intelligent and auto-mated operations, including automatic recognition of tobacco plant height, individual plant profiling, automatic adjustment of the cutting platform, automatic identification and positioning of apical buds, and precise application of sucker control agents.

Table 1

To meet the requirements of intelligent tobacco topping and the agronomic necessity of removing topped buds, leaves, and shoots from the field to prevent the spread of viruses and pathogens (*Ganguly et al., 2012, Belda-Palazon et al., 2022*), a reliable conveyor device compatible with standard tobacco topping machine frames was developed.

This device enables the integrated operation of topping, collection, and transportation, significantly reducing labour intensity, improving production efficiency, and supporting the expansion of tobacco field production.

The clamping and conveying device is a key component of the intelligent topping equipment, and its design quality directly affects its operational efficiency (*Fan et al., 2017, Zhou et al., 2025*). In response to the demand for a lightweight clamping and conveying device that can move rapidly along with the cutting equipment in existing intelligent cutting and topping devices, conducting research on a lightweight clamping and conveying device suitable for plant stems is of great significance (*Han et al., 2025*). Due to the varying diameters of tobacco top stalks, traditional clamping devices are often structurally complex and heavy, and thus cannot well meet the demand for rapid movement along with the cutting device. Therefore, this paper conducts the design and technical research on a lightweight clamping and conveying device suitable for flexible plant stems that can move rapidly with the cutting device. The dynamic simulation method, as an efficient and cost-effective approach, has been widely applied in the field of crop transportation by using computers to simulate and analyze the dynamic changes during actual clamping and conveying processes. Scholars worldwide have conducted dynamic simulation studies using ADAMS software on various plant stalks, including corn (*Li et al., 2024*), camellia oleifera (*Li et al., 2024*), sugarcane (*Zhong et al., 2022*), and chilli seedling (*Khadatkar et al., 2023*).

Considering the physical properties of tobacco top stalks and transportation requirements, we designed a lightweight clamping conveyor device by analying of the forces acting on key components and their operational principles. The ADAMS software was then used to simulate the clamping and conveying process of tobacco top stalks, conducting a rigid-flexible coupling dynamic analysis. Using clamping success rate and conveying success rate as evaluation indices, an orthogonal experiment with three factors (forward speed, clamping distance, and conveying speed) at three levels was conducted to optimize the working parameters of the lightweight clamping conveyor device. Field trials were then carried out to validate the findings, aiming to provide a reference for the research and optimization of intelligent topping devices.

MATERIALS AND METHODS

Physical and Mechanical Properties of Plants

Physical Characteristics of Plants

This article conducts the experiment using tobacco that requires topping. Tobacco variety used in this study was K326, and physical property measurements of well-matured tobacco top stalks were conducted in mid-June 2023 in Jukou Town, Jianyang District, Nanping City, Fujian Province. Field sampling was carried out using the five-point method, with 30 tobacco plants selected at each sampling point. The average values of the parameters were taken, and the main plant and field planting parameters are shown in Table 1.

Planting and plant characteristic parameters of tobacco

Parameter	Value
Plant height/mm	1230 ~ 1 460
Line spacing/mm	1200
Row spacing/mm	400~500
Stalk diameter at cutting point/mm	9.8 ~ 14.7
Diameter of stalk root /mm	25.9 ~ 28.4

Note: The stalk diameter at cutting point is the stalk diameter 30 mm down from the top of the tobacco.

Determination of Engineering Elastic Constants

The mechanical properties of tobacco top stalks are not isotropic. Considering the structural characteristics of tobacco top stalks, they can be classified as orthotropic materials with three mutually perpendicular elastic symmetry planes, and the material properties are transversely isotropic (*Zhou et al., 2013*).

The mechanical properties of orthotropic materials are characterized by nine engineering elastic constants, which represent the mechanical properties of each component: axial elastic modulus E_Z , radial elastic modulus E_X , E_Y . in-plane axial shear modulus G_{XY} , out-of-plane radial shear modulus G_{YZ} , G_{XZ} . in-plane Poisson's ratio μ_{XY} , and out-of-plane Poisson's ratios μ_{yz} , μ_{XZ} . Since the material properties of tobacco top stalks are transversely isotropic, the following relationships exist between the elastic constants:

$$\begin{cases} E_{X} = E_{Y} \\ G_{YZ} = G_{XZ} \\ \mu_{YZ} = \mu_{XZ} \\ G_{XY} = \frac{E_{X}}{2(1 + \mu_{XY})} \end{cases}$$
 (1)

The axial elastic modulus E can be obtained through tensile testing; the radial elastic modulus E_X can be obtained through radial compression testing. The shear modulus G_{YZ} can be determined through radial three-point bending testing. Tensile testing, radial compression testing, and radial three-point bending testing were all conducted in the laboratory of the Nanjing Institute of Agricultural Mechanization. The testing equipment used was the WDW-10 microcomputer-controlled electronic universal testing machine, with a measurement accuracy of $\pm 1\%$ and a maximum test force of 10 kN. The machine automatically controls the loading, unloading, and data collection and analysis. Other instruments used included testing fixtures, calipers, etc. The test samples were taken from the upper 300 mm segment of the tobacco top stalk, with the middle 160 mm segment of the stalk used as the specimen for determining the engineering elastic constants.

The experimental axial tensile elastic modulus of the tobacco top stalk was measured as E_Z =95.51MPa, while the calculated axial tensile elastic modulus of the stalk was E_Z =104.63MPa. The difference between the two is only 8.11%, indicating that the components of the tobacco top stalk along the axial direction exhibit composite material characteristics. Based on the study of the radial compression characteristics of tobacco top stalks, it can be inferred that the mechanical parameters of the tobacco top stalk's flexible body model can be set according to the elastic constants of the stalk. The elastic constants are shown in Table 2.

Tobacco stalk elastic constant

Table 2

Elasticity m	Elasticity modulus / MPa		Shear modulus / MPa		n ratio
E_X	0.73	G_{XY}	0.28	μχγ	0.30
E_Y	0.73	G_{YZ}	19.23	μγz	0.01
E_Z	95.51	G_{XZ}	19.23	μxz	0.01

Key Structural Design

Overall Structure and Working Principle

The entire intelligent tobacco topping machine is shown in Figure 1, and it mainly consists of the disc cutting device, clamping conveyor device, recognition and control system, power system, chassis, and other components.

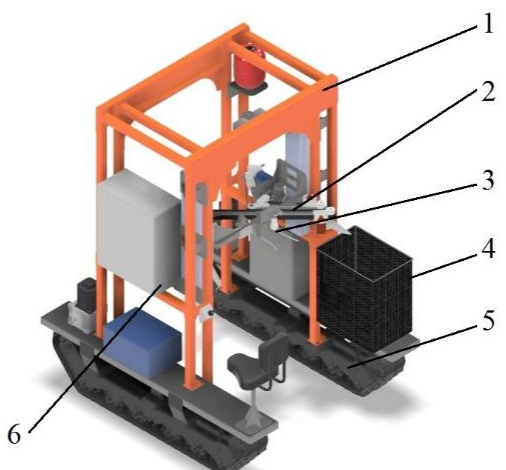


Fig.1 - Intelligent tobacco topping machine

1. Frame; 2. Clamping Conveyor Device; 3. Cutting Device; 4. Collection Bin; 5. Chassis; 6. Control System

The recognition system, clamping conveyor device, and disc cutting device are connected to the frame of the intelligent tobacco topping machine. The recognition system is installed at the front of the frame, while the disc cutting device and clamping conveyor device are mounted on the gantry frame, with both devices moving together with the gantry. The tracked chassis is powered by a lightweight and durable lithium battery; the control system can regulate the modules that control the vertical movement of the gantry motor and the operation of the disc cutting motor. The structure and performance parameters of the intelligent tobacco topping machine are shown in Table 3.

Machine structure and performance parameters

Table 3

Parameter	Value
Boundary dimension (Length×Width×Height) [mm×mm×mm]	1800×1420×2200
Overall quality / kg	610
Number of machine operation lines	1
Top height range [mm]	300
Theoretical operating speed [m·s ⁻¹]	0 ~ 0.8
Topping percent of pass [%]	≥90

During operation, as the topping machine moves forward, the recognition system detects the height of the tobacco plants and transmits the data to the control system. The control system then issues instructions to move the gantry vertically to the appropriate topping position. Subsequently, the tobacco top stalks are guided into the clamping conveyor device. After clamping, the disc cutting device cuts the tobacco top stalks. The clamping conveyor device continues to hold the cut tobacco top stalks and transports them to the collection bin, thereby completing the topping operation.

Clamping Conveyor Device Design Working Principle of the Clamping Conveyor Device

The clamping conveyor device mainly consists of a belt, driving pulleys, driven pulleys, tensioning pulleys, and a driving motor. As shown in Figure 2, to facilitate the transportation of the cut tobacco top stalks to the collection bin on the left rear side of the frame, the clamping conveyor device is deflected and suspended at an angle on the gantry frame, positioned at the front of the cutting disc, ensuring that the pulleys are in the same plane. For ease of installation and adjustment, two driving pulleys are symmetrically mounted at the end of the clamping guide device, with the driving motor mounted on the frame above the driving pulleys. The motor is connected to the driving shaft of the pulleys via a coupling. The left conveyor belt is a corner belt, with the left driven pulley suspended and installed at the front of the gantry frame. The tensioning pulley is installed on the inner side of the corner, and through the action of a screw tensioner, it keeps the tensioning pulley in constant contact with the clamping belt, pushing the belt inward to maintain tension. The right conveyor belt is a straight belt, with the driven pulley also performing tensioning through the screw tensioner. The conveyor belt is inclined at a certain angle, forming a V-shaped feeding entrance with the left corner belt. During operation, two in-dependent motors drive the driving pulleys to effectively clamp the tobacco top stalks between two vertically installed flexible clamping belts. The distance between the two clamping belts allows the tobacco top stalks to pass through. The spacing between the left and right split frame sections is adjustable, and combined with the flexible clamping belts, it can accommodate tobacco top stalks of varying diameters.

Subsequent design of the related conveyor belt structure and optimization of operational parameters can effectively reduce mechanical collision damage, while enhancing the stability and adaptability of the conveyor device.

Key Mechanism Design

The force analysis of the tobacco top stalk clamping is shown in Figure 2. When the stalk just enters the end of the V-shaped entrance, the following conditions must be met to ensure smooth feeding into the clamping inlet:

$$2 F_f \cos \alpha \ge 2 F_N \sin \alpha \tag{2}$$

where: α represents the angle between the clamping force and the line connecting the centers of the two synchronized pulleys, °; F_f is the frictional force between one side of the synchronized belt and the stalk, N. and F_N is the clamping force exerted by the synchronized belt on the stalk, N.

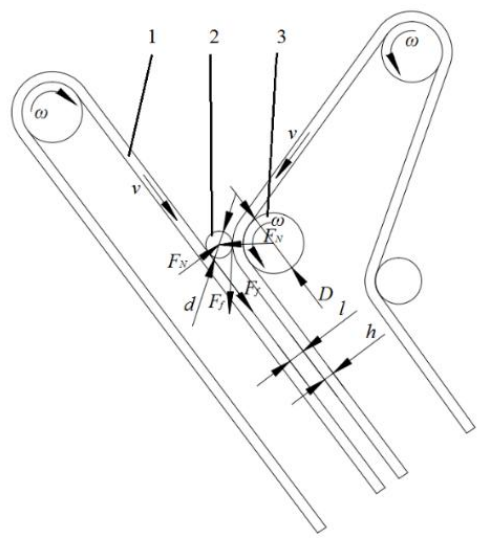


Fig. 2 - Clamping force analysis of tobacco top stalk
1. Clamping Conveyor Belt; 2. Tobacco Top Stalk; 3. Tension Pulley

The frictional force F_{ℓ} is equal to the product of the clamping force F_{N} and the coefficient of friction μ :

$$\mu \ge \tan \alpha$$
 (3)

According to the geometric relationship:

$$\cos\alpha = \frac{D+2h+1}{D+2h+d} \tag{4}$$

where: D represents the diameter of the synchronized pulley, mm; h is the thickness of the synchronized belt, mm; l is the gap between the synchronized belts, mm; and d is the diameter of the stalk at the clamping point, mm.

The compression ratio i of the synchronized belt on the stalk is expressed as:

$$i = \frac{d - l}{d} \tag{5}$$

Considering the compression ratio of the belt on the tobacco top stalk and the low-damage requirements for flexible synchronized belt clamping of the stalk, the compression ratio i is set to 0.3. Previous experiments showed that the average diameter at the cutting point of the tobacco top stalk was d=12.69 mm. Using the compression ratio formula, the gap I is calculated to be 8.18 mm. The coefficient of friction between the rubber belt and the tobacco top stalk was previously determined to be 0.35. Using the geometric relationship, the outer diameter of the synchronized pulley D is calculated as 54.76 mm. Given the larger external shape and high moisture content of the tobacco top stalk, some scattered outer leaves may be compressed during the clamping and transport process, which can reduce the frictional force as the moisture on the surface of the clamping belt increases. This may lead to slipping of the clamping belt or falling of the tobacco top stalk. A high-density flexible belt with a clamping surface width of 50 mm and a thickness of 8 mm is selected. The drive and driven pulleys are determined to be 15H synchronized pulleys with an outer diameter of 59.27 mm and a total pulley width of 55.4 mm, with a flange thickness of 1.5 mm. The minimum spacing between the two clamping belts is de-signed as 8 mm. The gap between the two belts affects the clamping force, and further tests are conducted to determine the optimal belt gap.

Clamping Conveyor Belt Design

According to the force analysis of the tobacco top stalk during the clamping and transport process (Fig.3), the following conditions must be met to ensure that the tobacco top stalk remains clamped and does not fall off:

$$\begin{cases}
f_{N1} \ge mg \\
f_{N1} = F_{N1} \cdot \mu_{N1}
\end{cases}$$
(6)

where: f_{NI} is the frictional force, N;

 F_{NI} is the normal force, N;

 μ_{N1} is the static coefficient of friction between the clamping belt and the tobacco top stalk; m is the mass of the tobacco top stalk, kg.

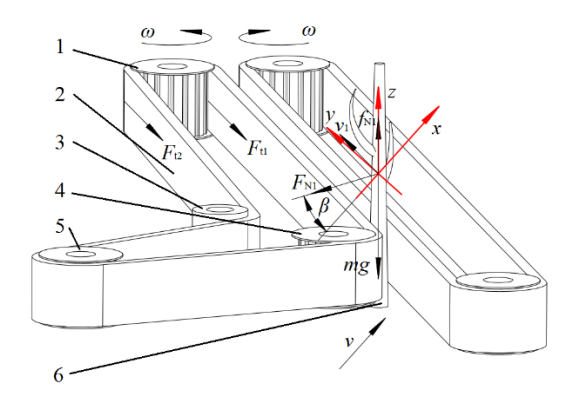


Fig. 3 - Clamping kinetic analysis of tobacco top stalk

1. Driving Pulley; 2. Clamping Belt; 3. Tension Pulley; 4. Directional Pulley; 5. Driven Pulley; 6. Tobacco Top Stalk

To prevent the clamping belt from slipping, the initial tension F_{θ} of the clamping belt after tensioning must satisfy:

$$\begin{cases}
F_0 = 500 \frac{P_c}{zv_1} \left(\frac{2.5}{K_\alpha} - 1\right) + qv_1^2 \\
v_1 = (F_{t1} - F_{t2})v_1
\end{cases}$$
(7)

where: F_0 is the initial tension of the conveyor belt, N; P_c is the transmission power, kW; z is the number of belt strands; K_a is the wrap angle correction factor; v_1 is the linear speed of the conveyor belt, m·s-¹; q is the mass per unit length of the clamping belt, kg·m-¹; F_{t1} and F_{t2} are the tension forces on the tight side and slack side of the clamping belt, respectively, N.

To achieve efficient clamping and transfer of the tobacco top stalks and prevent congestion at the feeding entrance, the linear speed of the clamping belt v_1 should be greater than the forward speed of the topping machine v_{m1} .

$$\begin{cases}
v_1 \ge \frac{v_m}{\cos \beta_1} \\
v_1 = \frac{\pi n_t D_1}{60}
\end{cases}$$
(8)

where: v_m is the forward speed of the topping machine, m·s⁻¹; β_1 is the angle between the clamping belt and the horizontal plane, °; D_1 is the diameter of the driving pulley, mm; n_t is the rotational speed of the driving pulley, r·min⁻¹.

According to equations (7) and (8), the transmission power of the clamping and guiding device is related to the length configuration of the working section, the rotational speed of the driving pulley, and the guiding angle of the device. The rotational speed of the driving pulley affects the speed at which the tobacco top stalks are clamped and transported, while the forward speed of the topping machine influences the speed at which the tobacco top stalks enter the clamping system. During tobacco top stalk clamping and transportation, the faster the forward speed v_m of the topping machine, the faster the tobacco top stalks enter the clamping system, since the plant spacing is fixed. If the forward speed v_m of the harvester is greater than the transport speed in the direction of the tobacco top stalk, the tobacco will not be transported in time, leading to continuous accumulation and eventually causing a blockage at the clamping belt entrance, halting further operation. However, if the forward speed of the harvester is less than the transport speed of the clamping belt, the tobacco top stalks will be clamped and transported in time, avoiding blockage and fulfilling the operational requirements. When the rotational speed n_t of the driving pulley increases, the linear speed v_t of the clamping belt increases, which helps improve the clamping and transport efficiency. However, to prevent tobacco top stalks from accumulating and causing blockages at the feeding entrance, it may be necessary to appropriately reduce the harvester's forward speed v_m and decrease the clamping belt angle β_1 .

Clamping Height Design

The clamping height is measured from the ground to the point where the clamping conveyor belt exerts force on the tobacco top stalk (*Zou et al., 2019*). During the topping process, the tobacco top may be tilted at a certain angle. The initial clamping position of the tobacco stalk and the height of the stalk's center of gravity after cutting determine the clamping success rate. If the clamping conveyor device effectively acts within the center of gravity range, reliable clamping of the tobacco stalk can be achieved. This is an important factor affecting the performance of the stalk clamping and conveying system.

Clamping point height calculation formula:

$$H = (h_1 + d_1 / \sin \gamma) \cdot \sin \gamma \tag{9}$$

where: γ is the angle between the force exerted by the cutter bar and the ground, °; h_1 is the length from the tobacco stalk clamping point to the cutting point, mm; d_1 is the height of the cutter bar from the ground, mm; and H is the clamping point height, mm.

During the clamping and conveying process, due to the uneven height of tobacco stalks and the presence of side branches on some stalks, the clamping point of the belt does not coincide with the center of mass of the tobacco stalk, resulting in a certain distance discrepancy. If the center of mass is above the clamping point (state A), the moment M exerted by the tobacco stalk's weight F on the clamping point causes the stalk to rotate around the belt clamping point, resulting in a deviation from the belt transport direction by a certain angle $(+\gamma)$, considered positive. At this point, the component force along the direction of the tobacco top stalk is F_1 , and the component force perpendicular to it is F_2 . Similarly, in the opposite state (state B), the tobacco stalk will shift towards the transport direction by a certain angle $(-\gamma)$, considered negative. If the center of mass coincides with the clamping point, the tobacco stalk will normally transition from being vertical to the horizontal ground to being vertical to the transport direction, i.e., $\gamma = 0$, at which point the tobacco stalk is perpendicular to the belt's transport direction. The analysis of the tobacco stalk's offset motion is shown in Figure 4.

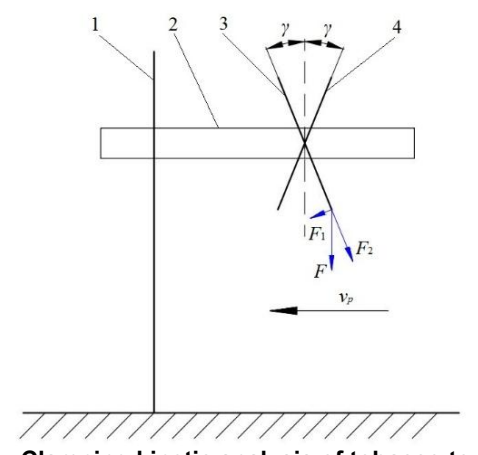


Fig. 4 - Clamping kinetic analysis of tobacco top stalk

1. Tobacco Top Stalk; 2. Conveyor Belt; 3. Forward-Shifted Tobacco Stalk; 4. Rearward-Shifted Tobacco Stalk

The relationship between the torque M and the offset angle γ , with force analysis shown in the figure 4.

$$M=F_1l \tag{10}$$

$$F = mg = m\pi r^2 l\rho \tag{11}$$

$$x = \frac{at^2}{2} = \frac{l_{AB}\sin\gamma}{\cos\gamma} = l_{AB}\tan\gamma \tag{12}$$

$$F_t = m\alpha = F\sin\gamma$$
 (13)

$$L=v_n t$$
 (14)

By solving equations (10) to (14) simultaneously, it obtains:

$$\gamma = \arctan\left(\frac{FL^2}{mlv_p^2}\right) \tag{15}$$

where: m is the mass of the tobacco apex in segments AB (AC), kg; ρ is the density of the tobacco top stalk, kg·m⁻³; v_p is the conveyor belt speed, m·s⁻¹; l_{AB} is the distance between the holding point and the centroid, m.

As shown in equation (15), during the belt clamping and conveying process, the tobacco top stalk starts in a vertical position and, under the action of torque, experiences a displacement. Therefore, the relative position between the belt clamping point (clamping height) and the tobacco top stalk's centroid, as well as the angle between the conveying mechanism and the ground, affect the displacement variation of the tobacco top stalk during the conveying process.

Key Component Simulation Model

Simulation Model of the Flexible Clamping Device

During the actual conveying process, the external forces acting on the tobacco stalk are difficult to measure directly. Therefore, this section combines SolidWorks, ANSYS, and ADAMS software to establish a rigid-flexible coupling model of the tobacco top stalk conveying mechanism and simulate the conveying process, in order to explore the influence of related factors on the clamping and conveying force experienced by the tobacco top stalk.

The clamping and conveying device were modeled in 3D using SolidWorks, and the established 3D model is shown in Figure 6. The structural parameters of the clamping and conveying device model were determined based on the previous operational parameters and theoretical analysis. The width of the drive and driven pulleys is 58mm, the width of the conveyor belt is 50mm, and the belt entry angle is 80°. The model mainly consists of two side belts, a drive pulley, a tension pulley, and a driven pulley, and does not include components unrelated to the clamping and conveying effect, such as nuts, bolts, and tension plates.

Establishment of the tobacco stalk model

The tobacco stalk simulation model in this study is based on tobacco. The dimensions, shape, and shape parameters of the tobacco stalk are determined based on preliminary statistical results. The model has a height of 300 mm, a taper of 0.03, and set up five group models of tobacco top stalk with cutting diameters at the cutting point of 10mm, 11mm, 12mm, 13mm, 14mm and 15mm respectively. The tobacco top stalk density of tobacco is 1080, and other physical parameters are shown in Table 2. The basic information of conveyor belt is shown in Table 4.

Material parameters

Table 4

Item	Poisson ratio	Elasticity modulus	Density	Yield strength	Shear modulus
	-	[MPa]	[kg•m ^{-3]}	[MPa]	[MPa]
Conveyor belt	0.45	7.84	7850	25	0.3

Model Flexibilization

The Parasolid format model imported directly into ADAMS is a rigid body model. If the tobacco stalk is modeled as a rigid body, it will not undergo any deformation during the simulation, which cannot reflect the real situation of the clamping and conveying process. Therefore, the flexible body model of the tobacco stalk is established using ANSYS.

Theory of Flexible Bodies

ADAMS represents the elasticity of an object through modes. This theory assumes that the elastic deformation of an object is a small deformation relative to the object's coordinate system, which itself undergoes large nonlinear overall movements and rotations. The basic idea is to assign a set of modes to the flexible body, use modal expansion methods, and represent the elastic displacement by a linear combination of modal vectors and modal coordinates. The deformation motion is described by calculating the elastic displacement of the object at each time step. The file generated by this method is an MNF file, which stands for Modal Neutral File. It can be used to establish an ADAMS flexible body system or a rigid-flexible coupled system.

Establishment of the Flexible Body MNF File

Import the Parasolid format file of the tobacco top stalk into ANSYS. First, define the material type of the model. For flexibility, select an appropriate element type from the element library (*Wang et al., 2017*). In this study, the SOLID185 element is selected for the flexible unit, with a material type of Orthotropic. After defining the element type, the material properties of the tobacco top stalk are defined based on previous mechanical performance test results.

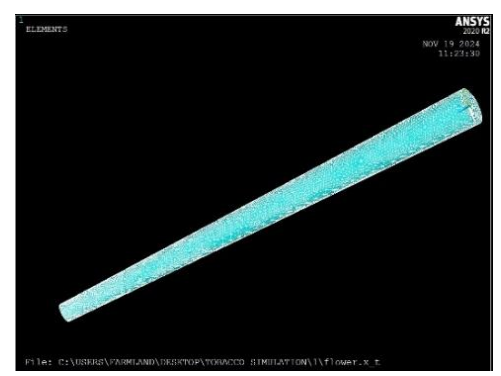


Fig. 5 - Mesh Division of the Tobacco Top Stalk

The meshing method for the stalk model uses the Smart Size method in ANSYS. The tobacco top stalk after meshing is shown in Figure 5. Next, rigid region connection points are created at the centers of both end faces of the stalk, and these points are then connected to the end faces to create rigid domains. Finally, the flexible body finite element model of the stalk is exported using the "Export to ADAMS" command.

Addition of Kinematic Pairs and Drives

Based on the principle of the conveying mechanism for holding and transporting the tobacco stalk, connection constraints between components and driving dynamics need to be added. Position the center marking points of each component. A revolute pair is set between the tensioner and the synchronous belt, a prismatic pair is set between the tensioner and the spring damper, a fixed pair is set between the synchronous belt support frame and the ground, and a force contact is added between the stalk and the two synchronous belts.

The straight belt is composed of 196 small units connected in series, and force contact is created between each small unit and the stalk. After adding the kinematic pairs, a drive is required to make the components move. In the belt system, the entire model is energized by adding a "belt excitation input," selecting the corresponding pulley system, conveyor belt system, and excitation pulley. The excitation type is set to torque, the function type is constant, and the driving torque is the product of the belt driving force and the radius of the driving pulley, with a value of 30 N/m.

Contact Addition

In ADAMS, the contact force is calculated in two ways: The first is a contact algorithm based on regression coefficients. ADAMS/Solver uses this algorithm to calculate the con-tact force with penalty parameters and regression coefficients. The penalty parameter imposes a unilateral constraint, and the regression coefficient determines the energy loss during contact; The second is a contact algorithm based on the collision function. ADAMS/Solver uses the Impact function from the ADAMS function library to calculate the contact force. The Impact function is composed of elastic force generated by the interaction between two objects and damping force generated by relative velocity. Before solving, the contact parameters need to be set. The Impact function works better under continuous contact conditions. Therefore, the Impact function method is used to define the collision contact force between the components of the conveyor mechanism and the tobacco stalk (*Li et al.*, 2023).

Determination of the stiffness coefficient

The stiffness coefficient k is determined by the following equation:

$$k = \frac{4\sqrt{\varphi}E^*}{3} \tag{16}$$

In the above equation, ρ and E^* can be calculated by the following equation:

$$\begin{cases}
\varphi = \varphi_1 \cdot \varphi_2 / (\varphi_1 + \varphi_2) \\
E^* = E_1 \cdot E_2 / [E_1 (1 - \mu^2) + E_2 (1 - \mu^2)]
\end{cases}$$
(17)

where: φ is the combined radius of curvature, mm; E^{\star} is the combined elastic modulus, MPa; φ_1 , φ_2 are the radius of curvature at the collision point between the conveyor belt and the tobacco top stalk, mm; E_1 , E_2 are the elastic moduli of the conveyor belt and the tobacco top stalk, respectively, MPa; μ_1 , μ_2 are the Poisson's ratios of the conveyor belt and the tobacco top stalk, respectively.

The stiffness coefficient between the tobacco top stalk and the synchronous belt is calculated to be 5.91N·mm⁻¹.

Determination of Collision Index

The collision index e was adopted from the recommended value in ADAMS, taken as 2.2.

Determination of the maximum damping coefficient

The recommended value of the maximum damping coefficient c_{max} in ADAMS is generally set to 0.1%-1% of the stiffness coefficient. In the Impact function, the damping coefficient is constant. For collisions between large mass objects, the recommended value can be used, while for collisions between small mass objects, the damping coefficient is set based on literature references. The maximum damping coefficient between the tobacco stalk and the conveyor belt is determined to be 0.0025.

Determination of penetration depth

The penetration depth is not the maximum penetration depth between objects. It is typically set to 0.1mm based on ADAMS recommended value. This penetration depth value does not limit further penetration between colliding objects when the damping reaches its maximum. Moreover, a smaller penetration depth allows the damping effect to quickly reach its maximum value after contact occurs. Additionally, the damping effect remains consistent during the contact process.

Determining the coefficient of friction and the translational speed

In the Impact function, the frictional force is determined by the Coulomb model, where the friction force is the product of the normal force acting on the object and the co-efficient of friction. The coefficient of friction can be divided into static friction coefficient μ s and dynamic friction coefficient μ d. Both are related to the material properties of the contacting bodies and the roughness of the surface. Based on previous measurements of the friction coefficient between the tobacco top stalks and the conveyor belt, the static and dynamic friction coefficients in the Coulomb model are determined to be 0.53 and 0.26, respectively.

After setting the contact parameters, the flexible body (MNF file) of the tobacco top stalk is substituted for the original rigid body file. The final tobacco top stalk-conveyor device coupled rigid-flexible model is shown in Figure 6.

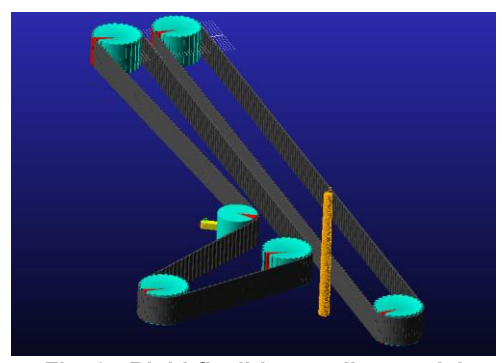


Fig. 6 - Rigid-flexible coupling model

Optimization Test Method Test Factors

The movement speed of the synchronous belt and the forward speed of the entire machine are the main factors influencing the variation in the resultant speed (*Shang et al., 2023; Zhang et al., 2020; Shi et al., 2018*). Based on preliminary tests, this study selects three factors—forward speed, belt holding gap, and belt conveying speed—as influencing factors. Three levels of holding gap distances, 8 mm, 12 mm, and 16 mm, were set within the range of holding distances; within the operational speed range of the topping machine, the forward speeds were set to 0.5 m/s, 0.65 m/s, and 0.8 m/s, based on the machine's movement; the belt conveying speeds were set to 0.8 m/s, 1.0 m/s, and 1.2 m/s. The experimental factors and their levels are shown in Table 5.

Test factors and levels

Table 5

Lovel	Forward speed	Clamping distance	Conveying speed	
Level [m·s·1]		[r·min ⁻¹]	[m·s ⁻¹]	
1	0.8	8	0.8	
2	1.0	12	1.0	
3	1.2	16	1.6	

Evaluation indicators

Currently, there is no experimental standard for tobacco topping and clamping transport. In this study, experimental indicators are set based on clamping and transport devices for vegetables (*Yang et al., 2021*), peanuts (*Chen et al., 2020*), and other crops (*Xin et al., 2023*). Simulations were conducted on tobacco top stalks of different diameters, and the results were averaged for statistical analysis.

Clamping success rate determination: In a stable working condition, the proportion of tobacco top stalks that are successfully drawn into the clamping guiding device, and without causing blockage or dropping within the measurement area. During the experiment, the number of effectively clamped tobacco top stalks must be determined.

Measurement is performed according to Equation (18), with five groups measured in total, and the results are averaged.

$$r_c = m_1 / m_2 \times 100\% \tag{18}$$

where:

 r_c represents the clamping success rate, %; m_1 is the number of effectively clamped tobacco top stalks; and m_2 is the number of cut tobacco top stalks.

Conveying success rate measurement: It refers to the proportion of tobacco top stalks that are conveyed by the device without any loss due to falling. During the experiment, the number of tobacco top stalks effectively conveyed must be measured.

A total of five groups were tested, and the average value of the results was taken.

$$r_t = n_1/n_2 \times 100\%$$
 (19)

where:

 r_t represents the conveying success rate, %; n_1 is the number of tobacco tops successfully transported; n_2 is the number of tobacco tops successfully clamped.

RESULTS

Simulation analysis of the clamping and transportation process

To obtain the instantaneous state of the tobacco top flower stalk during the simulation, a Marker point was established at the centroid of the stalk. Subsequently, within the Measure module of ADAMS, functions were employed to generate curves representing the force, velocity, and acceleration of the Marker point. When the forward speed is set to 1.1 m/s, the clamping gap is 12 mm, and the conveyor speed is 1.2 m/s, the ADAMS simulation contact force variation curve is shown in Figure 7. According to the simulation results, the clamping transport force does not exceed the breaking force of the tobacco stalk. When the clamping transport device first contacts the tobacco stalk, a large force change occurs, and then it remains in normal clamping transport. In the middle section, the belt undergoes significant deformation due to the tension, causing large fluctuations in the clamping transport force. Under the combined effect of friction and clamping force, it eventually stabilizes.

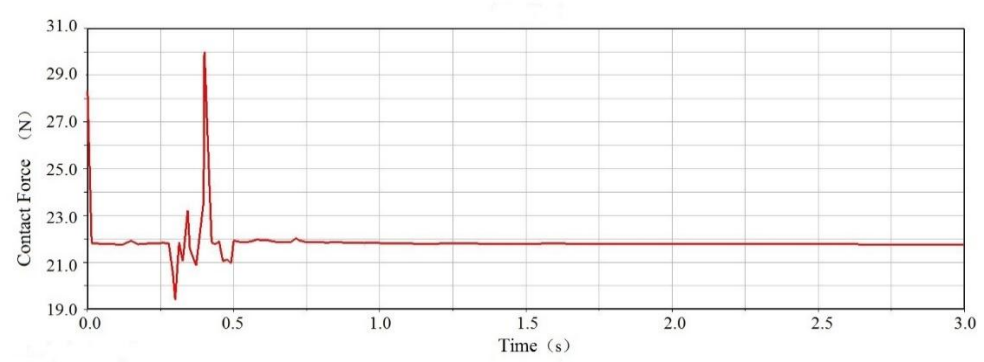


Fig. 7 - Contact Force-Time Curve

The change in the center of mass of the tobacco stalk reflects the clamping status. When the center of mass of the tobacco stalk undergoes a significant change in the *Z*-direction, it indicates that the tobacco stalk has fallen, meaning the clamping or conveying was unsuccessful. The change in the center of mass of the tobacco stalk is shown in Figure 8.

During the transportation process, the displacement of the tobacco stalk's centroid in the *Z*-direction did not show significant changes, indicating that the tobacco apex stalk was transported stably. The stalk moved 2mm in the *Z*-direction. The reason is that after the tobacco top stalk is held by the conveyor belt, it begins to move, and the reaction force from the tobacco stalk causes the belt to undergo elastic deformation in the forward direction. This elastic deformation provides space for the stalk to move slightly in the vertical direction. Particularly in the middle section of the transport, the centroid has a larger space for movement. Furthermore, the results indicate that the dynamic simulation with the tobacco top stalk defined as a flexible body better reflects the actual transportation conditions.

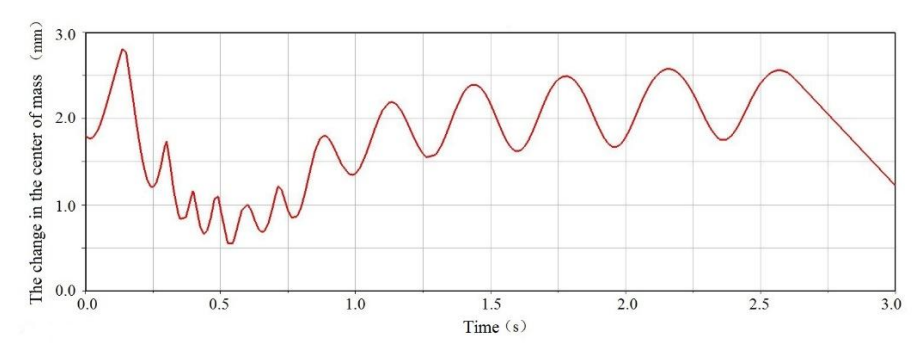


Fig. 8 - Center of Mass Diagram

Optimization Results and Analysis

The simulation experiment was conducted using a three-factor, three-level response surface analysis method. The influencing factors were forward speed x_1 , clamping distance x_2 , and conveyor belt speed x_3 , with evaluation indicators y_1 and cutting power consumption y_2 . A total of 17 simulation experiments were conducted, and the corresponding results for the evaluation indicators—clamping success rate and conveying success rate—are presented in Table 6.

Test design and results

Table 6

Serial number	Forward speed	Clamping distance	Conveyor speed	Clamping success rate y ₁	Conveying success rate y ₂
	[m·s ⁻¹]	[r·min ⁻¹]	[m·s ⁻¹]	[%]	[%]
1	1	12	1.2	92.96	94.52
2	1	16	1.6	93.76	94.78
3	1	12	1.2	94.61	97.6
4	1	8	0.8	94.75	97.24
5	1.2	8	1.2	92.21	92.17
6	1	8	1.6	92.13	91.62
7	1.2	16	1.2	92.14	90.58
8	0.8	16	1.2	92.66	95.78
9	1.2	12	0.8	94.29	97.96
10	0.8	12	1.6	94.77	97.91
11	0.8	12	0.8	94.93	97.44
12	1	12	1.2	91.75	91.75
13	1	12	1.2	92.86	95.63
14	1	16	0.8	95.12	98.24
15	1.2	12	1.6	93.78	94.66
16	0.8	8	1.2	92.89	91.64
17	1	12	1.2	92.53	92.65

The experimental results were analyzed using quadratic regression with Design-Expert 8.0.6 software. The analysis of variance results for clamping success rate y_1 and conveying success rate y_2 are shown in Table 7. The regression model equations for clamping success rate and conveying success rate were then fitted, and the effects of each factor and their interactions on the evaluation indicators were studied.

For the clamping success rate y_I and conveying success rate y_2 , the regression coefficients in the regression equations were tested using an F-test at a 0.05 confidence level. Non-significant terms were removed, and the resulting regression equations are as follows:

$$y_1 = +94.84 - 0.39x_1 - 0.42x_2 + 0.51x_3 + 0.39x_1x_2 - 0.28x_1x_3 - 0.91x_1^2 - 1.37x_2^2 - 0.74x_3^2$$
 (20)

$$y_2 = +97.69 - 0.85x_1 - 1.82x_2 + 0.39x_3 - 0.9x_1x_2 - 0.56x_2x_3 - 1.08x_1^2 - 4.35x_2^2 - 0.63x_3^2$$
 (21)

By combining Formula (20) with the variance analysis table, it can be concluded that the model is highly significant (P<0.0001), indicating a good fit. The lack-of-fit term is not significant (P=0.7284>0.05), indicating no lack-of-fit factors, which suggests that the regression model can be used as a substitute for real experiments. Analyzing the results, the first-order terms x_1 , x_2 , x_3 , the interaction term x_1x_2 , and the quadratic terms x_{12} , x_{22} , x_{32} have a highly significant impact on the clamping success rate. The interaction term x_1x_3 significantly affects the clamping success rate. The influence of factors on the clamping success rate is ranked as: conveyor speed > clamping distance> forward speed.

From Formula (21) combined with the analysis of variance table, it can be concluded that the model is highly significant (P<0.0001), indicating a good model fit. The lack-of-fit term is not significant (P=0.7929>0.05), indicating no lack-of-fit factors, which suggests that this regression model can replace the real experiment. The first-order terms x_1, x_2 , the interaction term $x_2 x_3$, and the quadratic terms x_{12}, x_{22}, x_{32} have a highly significant effect on the transport success rate. The first-order term x_3 and the interaction term $x_2 x_3$ have a significant effect on the transport success rate. The influence of factors on the transport success rate is ranked as: clamping distance > forward speed > conveyor speed.

Variance analysis of regression equation

Table 7

	Clamping success rate y ₁ /%			Conveying success rate y ₂ /%				
Source	Sum of Squares	Degree of freedom	F value	allie i Pvallie i	Sum of Squares	Degree of freedom	F value	P value
Model	20.70675 5	9	78.85	< 0.0001**	111.9439	9	110.57	< 0.0001**
X 1	1.193512 5	1	40.90	0.0004**	5.81405	1	51.68	0.0002**
X 2	1.419612 5	1	48.65	0.0002**	9.396113	1	83.53	< 0.0001**
Х3	2.10125	1	72.02	< 0.0001**	1.193513	1	10.61	0.0139*
X ₁ X ₂	0.6241	1	21.39	0.0024**	0.525625	1	4.67	0.0674
X ₁ X ₃	0.319225	1	10.94	0.0130*	3.222025	1	28.64	0.0011**
X 2 X 3	0.002025	1	0.069	0.7998	1.2544	1	11.15	0.0124*
X ₁₂	3.452338	1	118.32	< 0.0001**	4.915706	1	43.70	0.0003**
X 22	7.850906	1	269.07	< 0.0001**	79.60044	1	707.61	< 0.0001**
X 32	2.293238	1	78.60	< 0.0001**	1.687112	1	15.00	0.0061**
Residual	0.204245	7			0.787445	7		
Lack of fit	0.051925	3	0.45	0.7284	0.163525	3	0.35	0.7929
Pure error	0.15232	4			0.62392	4		
Total	20.911	16			112.7314	16		

Note: P<0.01 (highly significant**); P<0.05(significant*).

Response Surface Analysis of Each Factor

Response surface and contour plots are used to analyze the influence of the clamping gap, conveyor belt speed, and forward speed on the evaluation Indicators.

Figure 9a shows the response surface plot of the interaction between conveyor belt speed and forward speed on clamping success rate when the conveyor belt speed is at the middle level. From Figure 9a, it can be observed that under the same clamping distance, the clamping success rate first increases and then decreases as the forward speed in-creases. The main reason is that under a suitable clamping gap, with the increase in for-ward speed, the transportation process becomes smoother, and the clamping entrance is not congested, resulting in a higher clamping success rate.

As the forward speed continues to increase, the number of tobacco top stalks increases, which may cause congestion at the clamping entrance, affecting the clamping success rate. Under the same forward speed, the clamping success rate first increases and then decreases as the clamping gap increases. This is mainly because, under a suitable forward speed, as the clamping gap increases, larger diameter tobacco stalks can smoothly enter the clamping channel with guidance, improving the clamping success rate. However, when the clamping gap increases beyond a certain value and becomes larger than the tobacco stalk diameter, the tobacco top stalks are not easily able to enter the clamping channel, leading to congestion in severe cases and a decrease in clamping success rate.

Figure 9b shows the response surface plot of the interaction between conveyor belt speed and clamping gap on clamping success rate when the forward speed is at the middle level. From Figure 9b, it can be seen that at a certain forward speed, the clamping success rate first increases and then decreases as the conveyor belt speed increases. The main reason is that with the increase in conveyor belt speed, the already clamped tobacco tops are quickly transported through the clamping channel, leading to a higher clamping success rate. However, when the conveyor belt speed is too high, the relative speed difference between the stalk and the belt becomes large, causing the tobacco stalk to easily fall off, which results in a lower clamping success rate.

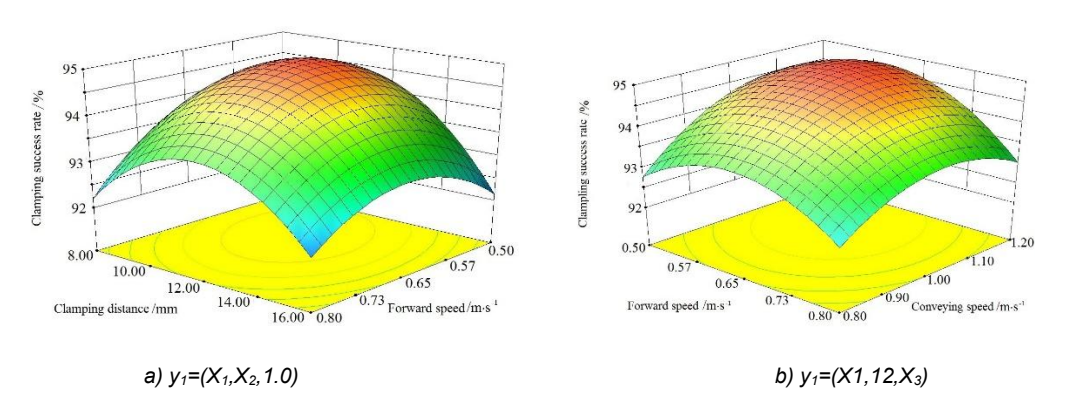


Fig. 9 - Influence of interactive factors on clamping success rate

Figure 10a shows the response surface plot of the interaction between conveyor belt speed and clamping gap on delivery success rate when the clamping gap and forward speed are at the middle levels. From Figure 10a, it can be observed that under the same forward speed, the delivery success rate increases slowly as the conveyor belt speed in-creases.

The main reason is that under a suitable clamping gap, the increase in conveyor belt speed leads to a smoother and more stable transportation process, which increases the delivery success rate. As the forward speed continues to increase, the tobacco top stalk delivery amount increases, but excessive deformation of the conveyor belt leads to poor stability, reducing the delivery success rate. Under the same conveyor belt speed, the delivery success rate slowly decreases as the delivery speed increases. This is mainly because when the conveyor belt speed is too high, the vibrations caused by the conveyor belt cause significant changes in the clamping gap, leading to poor delivery stability.

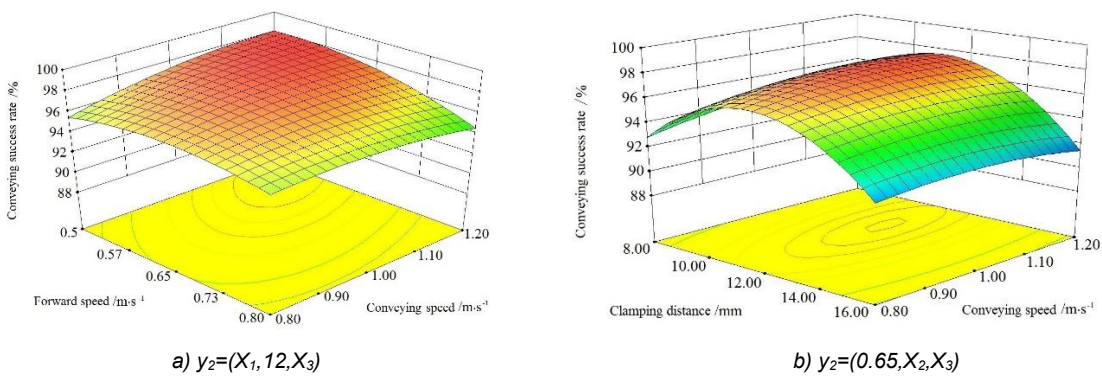


Fig. 10 - Influence of interactive factors on conveying success rate

Figure 10b shows the response surface plot of the interaction between conveyor belt speed and clamping gap on delivery success rate when the forward speed is at the middle level. From Figure 10b, it can be concluded that under a certain conveyor belt speed, the delivery success rate first increases and then decreases as the clamping gap increases. The main reason is that under a certain conveyor belt speed, as the clamping gap increases, the transportation process becomes smoother, allowing larger diameter tobacco stalks to be stably transported, which improves the delivery success rate. However, when the clamping gap becomes too large, tobacco tops may flip or slip during the transportation process, reducing the stability and reliability of stem delivery, thus lowering the clamping success rate.

Parameter Optimization and Validation

Parameter Optimization

In order to achieve the optimal conveying performance of the lightweight clamping and conveying device (*Cai et al., 2020*), the optimization module in Design-Expert 8.0.6.1 software was used to optimize and solve the regression model (*Li et al., 2022; Sidahmed et al., 2004*), with the following constraints:

$$\begin{cases}
\min y_1(x_1, x_2, x_3) \\
\min y_2(x_1, x_2, x_3) \\
0.8 \le x_1 \le 1.2 \\
8 \le x_2 \le 16 \\
0.8 \le x_3 \le 1.6
\end{cases} \tag{22}$$

The optimal cutting operation parameters were obtained by optimizing the objective function: the forward speed is 0.58 m/s, the clamping gap is 11.22 mm, and the conveying speed is 1.10 m/s. Under these conditions, the clamping success rate is 95.03% and the conveying success rate is 98.22%.

Verification Test Conditions

To verify the actual operational performance of the tobacco topping and conveying device, a performance test was conducted in June 2023 in Jukou Town, Jianyang District, Nanping City, Fujian Province. The average tobacco planting row spacing was 1200 mm, and the plant spacing was 500 mm. The tobacco variety was K236, with an average plant height of 1193.7 mm, and the average stalk diameter at the topping point was 12.69 mm. The field of the topping test is shown in Figure 11.



Fig. 11 - Field test

Other auxiliary tools included an electronic scale (manufactured by Shanghai Lichen Instrument Technology Co., Ltd., model: YP300001D, range: 0-30 kg, accuracy: 0.1 g), a vernier caliper, a tape measure (0-150 m), and a stopwatch.

Experimental verification results

According to the comprehensive balance method, since the factors significantly affect the gripping success rate, transport success rate, and economic benefits, the optimal combination parameters were selected: a forward speed of 0.6 m/s, a gripping distance of 11 mm, and a transport speed of 1.1 m/s. Field verification tests were conducted with three repetitions, and the results are shown in Table 8.

Test verification results

Table 8

Toyd No	Clamping success rate y ₁	Conveying success rate y ₂		
Text No.	[%]	[%]		
1	93.96	98.05		
2	94.82	98.63		
3	94.78	98.41		
Average value	94.52	98.36		

The verification test results show that when the forward speed is 0.6 m/s, the gripping distance is 11 mm, and the transport speed is 1.1 m/s of the tobacco topping machine, the average gripping success rate is 94.52% and the average transport success rate is 98.36%.

Through experimental verification, the field test data was compared with the simulation results. The analysis shows that the average experimental results are in good agreement with the simulation results, with an error within 5%, confirming that the simulation model is valid and reasonable.

Discussion

ADAMS was used to conduct a flexible-body coupling dynamics simulation of the tobacco top stalk clamping and conveying process. The verification results show that this simulation method can explicitly model the dynamics of the lightweight clamping and conveying process, providing a new approach for the study of stalk- clamping and conveying processes.

This simulation method is effective in studying the impact of clamping and conveying device structural parameters on clamping success rate and conveying success rate, offering a viable approach for further optimization of structural parameters in the design of lightweight clamping and conveying devices, thereby shortening the development cycle of the clamping and conveying device. Based on the physical properties of the tobacco top stalk, a lightweight clamping and conveying device was designed. Due to its light weight, it can be fixed to the topping knife frame and move simultaneously with the cutting blade. It adapts to flexible clamping and conveying after plants of varying heights, improving the clamping and conveying success rate. In conclusion, the lightweight stalk clamping and conveying device designed in this study provides a smooth conveying process and high stalk collection rate. It can be paired with an intelligent topping machine with automatic height adjustment for the cutting table, offering good adaptability to planting agronomy. The functions of the components and operational performance meet the design expectations, fulfilling the fieldwork requirements for stalk topping.

CONCLUSIONS

By measuring the physical properties of stalks and determining the dynamic and static friction coefficients, a theoretical analysis of the key mechanisms of the lightweight top stalk clamping and conveying device was conducted. The effects of key operational parameters and structural parameters of the conveying device were clarified, and a light-weight stalk clamping and conveying device that can move with the topping device was designed.

The results from the dynamics simulation indicate that forward speed, clamping distance, and conveyor speed have a highly significant impact on clamping success rate and conveying success rate. Multi-objective optimization of the model was performed, and the optimal parameters were found to be a forward speed of 0.58 m/s, a clamping distance of 11.22 mm, and a conveyor speed of 1.10 m/s. Under these conditions, the clamping success rate is 95.03%, and the conveying success rate is 98.22%.

The clamping success rate and conveying success rate obtained from field trials were compared with the simulation results. The simulation optimization and field trial results are in good agreement, indicating that the ADAMS flexible-body coupling simulation method can be used for studying tobacco clamping and conveying devices, providing support for the development of such devices.

ACKNOWLEDGEMENT

This research was funded by the Central Public-Interest Scientific Institution Basal Research Fund (S202306); Agricultural Science and Technology Innovation Program of Chinese Academy of Agricultural Sciences (CAAS-ASTIP-31-NIAM-05); Science and Technology Program of Nanping Branch of Fujian Tobacco Company (NYK2023-08-03).

REFERENCES

- [1] Belda-Palazon, B., Costa, M., Beeckman, T., Rolland, F., Baena-Gonalez, E., (2022). ABA represses TOR and root meristem activity through nuclear exit of the SnRK1 kinase. *Proceedings of the National Academy of Sciences of the United States of America*, Vol. 119, No. 28, Article: e2204862119, Ghent/Belgium.
- [2] Cai, J., Zhang, J., Yeerbolati Tiemuer., Hao, Z., Rui, Z., (2020). Design and test of clamping belt cotton straw harvester (夹持带式棉秆收获机设计与试验). *Transactions of the Chinese Society of Agricultural Engineering*, Vol. 51, No. 10, pp. 152-160, Xinjiang/China.
- [3] Chen M., Zhai, X., Zhang, H., Yang, R., Wang, D., Shang, S., (2020). Study on control strategy of the vine clamping conveying system in the peanut combine harvester[J]. *Computers and electronics in agriculture*, Vol. 178, pp. 105744, Article 105744, Shandong/China.
- [4] Du, Y., Shi, S., Liu, H., Zhao, J., Ren, Z., He, P., Luo, X., Hang, X., (2019). Design of Hand-held Electric Tobacco Topping and Sprout Suppression System (手持式电动烟草打顶抑芽系统的设计). Journal of Agricultural Mechanization Research, Vol. 41, No. 12, pp.86-91, Chongqing/China.
- [5] Fan, G., Yang, Q., Zhang, X., Wang, J., Chen, R., (2017). Design and Test of Intelligent Tobacco Topping Machine with Clamping Belt (烟草夹持式智能打顶机设计与试验). *Transactions of the Chinese Society for Agricultural Machinery*, Vol. 48, No. 7, pp.121-126, Shandong/China.
- [6] Ganguly, A., Sasayama, D., Cho, H., (2012) Regulation of the polarity of protein trafficking by phosphorylation. *Molecules and cells*, Vol. 33, No.5, pp. 423-430, Seoul/Korea.
- [7] Geng, A., Zhang, X., Miao, N., Ma, M., Song, T., (2010). Development of 3YDX-3 topping and restraingerminating machine of tobacco (3YDX-3 型烟草打顶抑芽机设计). Transactions of the CSAE, Vol. 26, No. 7, pp.96-101, Shandong/China.
- [8] Gravalos, I., Ziakas, N., Loutridis, S., Gialamas, T., (2019). A mechatronic system for automated topping and suckering of tobacco plants. Computers and Electronics in Agriculture, Vol. 166, Article:1-11, Larissa/Greece.
- [9] Han, C., Liu, Z., Xu, Y., You, J., Qiu, S., (2025). Design and test of double-roller clamping type cotton topping device (双辊夹持式棉花打顶装置设计与试验). *Transactions of the Chinese Society of Agricultural Engineering*, Vol. 41, No. 11, pp. 455-465, Xinjiang/China.
- [10] Khadatkar, A., Pandirwar, A., Paradkar, V., (2022). Design, development and application of a compact robotic transplanter with automatic seedling picking mechanism for plug-type seedlings. *Scientific Reports*, Vol. 13, No. 1, pp. 1883, London/UK.
- [11] Lei, B., Chang, W., Zhao, H., Zhang, K., Yu, J., Yu, S., Cai, K., Zhang, J., Lu, K., (2022). Nitrogen application and differences in leaf number retained after topping affect the tobacco (Nicotiana tabacum) transcriptome and metabolome. *BMC Plant Biology*, Vol. 22, No. 1, Article 38, Chongqing/China.
- [12] Li, T., Wei, X., Jiang, W., Li, N., Zhang, H., (2022). Test Bench Study on Harvesting Characteristics of Sweet Potato Vines (甘薯秧蔓收获特性试验装置研究). *Transactions of the Chinese Society for Agricultural Machinery*, Vol. 53, No. S1, pp. 166-175, Shandong/China.
- [13] Li, X., Wang, M., Liu, Y., Pan, Y., Sun, P., (2023). Contact Modeling and Simulation Analysis on the Non-explosive Separation Device of a Spacecraft (航天器非火工分离装置接触建模与仿真分析). *Journal of Vibration and Shock*, Vol. 42, No. 06, pp. 298-306, Nanjing /China.
- [14] LI, X., Zhao, Y., Zhao, H., Li, S., Diao, P., (2024). Design and Testing of a Gap Adjustable Elastic Low Damage Corn Picking Header Based on ADAMS. *INMATEH-Agricultural Engineering*, Vol. 74, No. 3, pp. 388-430, Shandong/China.

- [15] LI, Z., Tang, L., Wu, M., Zhang, S., Zhang, H., (2024). Design and test of the fruit collecting device of camellia oleifera with angular scissor mechanism (偏移剪叉式油茶果收集装置设计与试验). *Transactions of the Chinese Society of Agricultural Engineering*, Vol. 40, No. 3, pp.62-71, Hunan/China.
- [16] Liu, S., Li, W., Wang, J., Qi, W., Zhang, X., Zhang, H., (2016). Design and Test of Testing Control System for Double Rows Intelligent Tobacco Topping Machine (双行智能烟草打顶抑芽机检测控制系统设计与试验). Transactions of the Chinese Society for Agricultural Machinery, Vol. 47 No. 6, pp.47-52, Shandong/China.
- [17] Luo, H., Zhang, S., Wu, M., Wang, C., He, J., Jiang, X., (2023), Design and Test of Soil-banking Machine with Centralized Soil Feeding and Double-sided Lateral Delivery for Tobacco (中间集抛后送式双侧斜输烟草培土机设计与试验). *Transactions of the Chinese Society for Agricultural Machinery*, Vol. 54, No. 120, pp.97-108,165. Hunan/China.
- [18] Shang, J., Ma, Y., Teng, D., Li, H., Lv, Z., (2023). Design and Test of Red Adzuki Bean Clamping Harvesting Device (红小豆夹持式收获装置的设计与试验). *Journal of Agricultural Mechanization Research*, Vol. 41, No. 12, pp. 134-139, Heilongjiang/China.
- [19] Shi, Y., Zhang, Y., Wang, X., Xun, J., (2018). Development and prototype experiment of environmental self-propelled and orderly harvester for Artemisia selengensis (环保自走式芦蒿有序收获机的研制与样机试验). *Journal of Chinese Agricultural Mechanization*, Vol. 39, No. 11, pp. 17-21, Nanjing /China.
- [20] Sidahmed, M.M., Jaber, N.S., (2004). The Design and Testing of a Cutter and Feeder Mechanism for the Mechanical Harvesting of Lentils[J]. *Biosystems Engineering*, Vol. 88, No. 3, pp. 295-300, Beirut/American.
- [21] Wang, D., Cheng, D., Wang, S., Chen, Z., Zhang, F., (2017). Analysis on Vibratory Harvesting Mechanism for Trained Fruit Tree Based on Finite Element Method (基于有限元方法的整形果树振动收获机理分析). *Transactions of the Chinese Society of Agricultural Engineering*, Vol. 33, No. S1, pp. 56-62, Beijing/China.
- [22] Worsham, A.D., Burch, T, B. (2002). Method an apparatus for simultaneously topping tobacco and controlling suckers with chemicals applied to cut stems by mechanical means. *USPTO Issued Patents*, 6446420, 2002-09-10.
- [23] Xin, S., Zhao, W., Shi, L., Dai, F., Feng, B., (2023). Design and experiments of the clamping and conveying device for the vertical roller *type* corn harvesting header (立辊式玉米收获割台夹持输送装置设计与试验). Transactions of the Chinese Society of A*gricultural Engineering*, Vol. 39, No. 9, pp. 34-43, Gansu/China.
- [24] Xia, Z., Chen L., Peng, Y., (2017). Study on Portable and Simple Control System of Tobacco Topping and Sucker Machine (轻简式烟草打顶抑芽机控制系统研究). *Journal of Anhui Agriculture Science*, Vol. 45, No. 24, pp.221-223, Zunyi/China.
- [25] Yang, Q, Ahmad Ibrar, Faheem Muhammad, Siddique Bushra, Xu Hu, Addy M., (2021). Development and assessment of belt-drive seedlings transmission device for fully-automatic vegetable transplanter[J]. *Computers and electronics in agriculture*, Vol. 182, pp.105958, Article 105958 Zhenjiang/China.
- [26] Zhang, T., Li, Y., Song, S., Pang, Y., Shao, W., (2020). Design and Experiment of Tumorous Stem Mustard Harvester Based on Flexible Gripping (基于柔性夹持的青菜头收获机设计与试验). *Transactions of the Chinese Society for Agricultural Machinery*, Vol. 51, No. S2, pp. 162-169, 190, Chongqing/China.
- [27] Zhong, J., Tao, Li., Li, S., Zhang, B., Wang, J., He, Y., (2022). Determination and interpretation of parameters of double-bud sugarcane model based on discrete element. *Computers and Electronics in Agriculture*. Vol.203, pp. 107428, Article 107428, Nanning/China.
- [28] Zhou, J., Fu, M., Chen, J., Cui, J., (2025). Design and Test of a clamping-shear intea-row weeding device. *INMATEH-Agricultural Engineering*, Vol. 75, No. 1, pp. 45-56, Harbin/China.
- [29] Zhou, Y., Li, X., Shen, C., Tian, K., Zhang, B., Huang, J., (2016). Experimental analysis on mechanical model of industrial hemp stalk. *Transactions of the Chinese Society of Agricultural Engineering*, Vol. 32, No. 9, pp. 22-29, Nanjing/China.
- [30] Zou, L., Liu, X., Li, J., Niu, Z., Song, Y., Yuan, J., (2019). Clamping Conveyer Device of Ordered Spinach Harvester Based on Rheological Property Analysis (基于流变特性分析的菠菜有序收获机夹持输送装置研究). *Transactions of the Chinese Society for Agricultural Machinery,* Vol. 50, No. 10, pp. 72-79, Shandong/China.